Biosensors and Bioelectronics 49 (2013) 318–322

Contents lists available at SciVerse ScienceDirect

Biosensors and Bioelectronics

journal homepage: www.elsevier.com/locate/bios

Short communication

Synthesis of mesoporous multiwall ZnO nanotubes by replicating silk and application for enzymatic biosensor

Minggang Zhao [a], Zhenglong Li [a], Ziqi Han [a], Ke Wang [a], Yu Zhou [a], Jingyun Huang [a,b,*], Zhizhen Ye [a,b,**]

[a] Department of Materials Science and Engineering, State Key Laboratory of Silicon Materials, Zhejiang University, Hangzhou 310027, China
[b] Cyrus Tang Center for Sensor Materials and Applications, Zhejiang University, China

ARTICLE INFO

Article history:
Received 22 March 2013
Received in revised form
4 May 2013
Accepted 14 May 2013
Available online 23 May 2013

Keywords:
ZnO
Mesoporous multiwall nanotubes
Glucose oxidase
Electrochemical biosensor

ABSTRACT

A facial biotemplate-directed synthetic route for fabricating mesoporous multiwall ZnO nanotubes (ZnO-MMNTs) was proposed. Owing to the mesoporous multiwall based matrix, one dimensional (1D) tubes based channels and high isoelectric point (IEP), the prepared ZnO-MMNTs are wonderful platform to immobilize glucose oxidase (GOx) for glucose biosensing. Scale-adaptive cells are constructed to hold enzymes molecules, maintain enzymatic activity and keep stability. The prepared enzymatic electrode (chitosan/GOx/ZnO/Au) exhibits high sensitivity (47.2 μA mM^{-1} cm^{-2}), very fast response (< 2 s), quite low K_M^{app} (1.09 mM), excellent selectivity and stability. Therefore, ZnO-MMNTs are promising material for enzyme assembly and other biological applications.

1. Introduction

Organisms in nature have unique and irreplaceable characteristics. Abundant micro- to nanostructures in biological systems can be found in nature. Therefore biological systems provide an ideal environment for synthesizing natural minerals with control of morphology and crystal structure (Belcher et al., 1996; Cha et al., 2000; Naik et al., 2002; Nuraje et al., 2006). In fact, inorganic structures replicated from biological templates may combine the merits offered by both the material and biological structures, and present excellent performances in photonics, catalysis, sensing and other fields (Huang et al., 2006; Becerril et al., 2005; Fatemi et al., 2012; Nuraje et al., 2012). Expanding biological synthesis to non-natural materials has thus been the focus of recent studies (Dickerson et al., 2008; Selbach et al., 2007; Brutchey et al., 2006; Tao et al., 2010).

Detection of glucose is important for clinical diagnosis, biological analysis, environmental monitoring, and food processing industries (Kong et al., 2009; Rakow and Suslick, 2000), so it is necessary to develop effective methods for its measurement. The enzymatic amperometric biosensors based on glucose oxidase (GOx) have been paid much attention due to the specificity of enzyme (Lee et al., 2005; Luo et al., 2004; Zhao et al., 2005). However, GOx immobilized on the bare solid electrode is difficult to achieve its activity and stability (Riklin et al., 1995; Fang et al., 2011). Searching for new materials for immobilizing enzymes is still very important for developing more active and stable biosensors. Nanostructured materials are promising to achieve this goal, due to their large specific surface, desirable microenvironment and special optical and electrical performance. Considering the size of the enzyme molecule and the need of suitable environment for maintaining its activity, the design of nanomaterials with controlled morphology and structure is crucial. Multi-walled carbon nanotubes allowed for efficient mobilization of the glucose oxidase (Xie et al., 2007). Porous hydrogel can provide three-dimensional porous nanostructures for stable enzyme immobilization and get excellent biosensing performance (Pan et al., 2012; Zhai et al., 2013). Because enzyme molecule contains lots of secondary branched structure, the need of extending room is important for maintaining its activity (Chi et al., 1994; Deng et al., 2007). Pores can act as cells to affer the required room. As we know, the introduction of small pores will increase the specific surface area of the materials. However, too small pores cannot hold the enzyme molecule and will prevent the fast diffusion of reactants (Heller, 1990). Therefore, the control of the nanostructure with suitable pores for holding enzymes and one dimensional (1D) channels for electrons and reactants transport are desirable for fabrication of biosensors. Comprehensive considering the above factors, the mesoporous 1D nanomaterials provide often the best compromise.

ZnO is an attractive semiconductor material with wide direct band gap (3.37 eV), large exciton binding energy (60 meV), and has promising application in optics, optoelectronics, sensors

* Corresponding author at:Department of Materials Science and Engineering, State Key Laboratory of Silicon Materials, Zhejiang University, Hangzhou 310027, China.
Tel.: +86 571 87952118; fax: +86 571 87952625.
** Corresponding author.
E-mail addresses: huangjy@zju.edu.cn, yezz@zju.edu.cn (J. Huang).

0956-5663/$ - see front matter © 2013 Elsevier B.V. All rights reserved.
http://dx.doi.org/10.1016/j.bios.2013.05.017

and actuators (Lei et al., 2011). Because of its biocompatibility, non-toxicity, electrochemical activities and fast electrical communication features, ZnO has shown novel advantages for the fabrication of enzymatic amperometric biosensors (Zhu et al., 2007; Singh et al., 2007; Zang et al., 2007). More importantly, ZnO with a high isoelectric point (IEP~9.5) is suitable for the adsorption of proteins with low IEP such as GOx (IEP~4.2) by electrostatic interaction (Zhai et al., 2011). Therefore, ZnO nanostructures are promising materials in application of biosensors.

In this work, biomorphic 1D mesoporous multiwall ZnO nanotubes (ZnO-MMNTs) were synthesized by replicating silk. As a biotemplate, silk is very easy to be obtained and cheap. The as-prepared ZnO-MMNTs with mesoporous multilayer walls are wonderful platform to immobilize GOx for glucose biosensing. The nanostructures possess size-adaptive mesoporous environment for enzyme loading and excellent gas and water-permeability for substrates and products to diffuse in and out. It not only maintains the strong adsorption and the activity of GOx, but also provides large tubes for fast diffusion of reactants and 1D channels for electronic transport. The as-fabricated biosensor has high sensitivity, fast response and good operational stability for glucose detection.

2. Materials and methods

2.1. Reagents and instruments

Glucose oxidase (100–250 U mg^{-1}) was purchased from Sigma. Chitosan (CHIT) (deacetylation value≥95%) was purchased from Aladdin-reagent. Zinc nitrate ($Zn(NO_3)_2 \cdot 6H_2O$), sodium dihydrogen phosphate ($NaH_2PO_4 \cdot 2H_2O$), disodium hydrogen phosphate ($Na_2HPO_4 \cdot 12H_2O$). Other reagents were purchased from Chemical Reagent Company of Shanghai and all of them were analytically pure.

The obtained sample was characterized by SHIMADZU 6000 X-ray powder diffraction (XRD) with Cu Kα radiation. The Raman scattering spectroscopy was measured with the Ar^+ (514.5 nm) as the excitation sources. The morphology and size of as-synthesized samples were characterized with SU-70 scanning electron microscopy (SEM). All the electrochemical experiments were performed with a WPG100e electrochemical workstation (Korea) at room temperature. The three electrodes system was adopted for measurement, consisting of the as-prepared GOx modified electrode as working electrode, a Pt electrode as counter electrode, and an Ag/AgCl electrode as reference electrode.

2.2. Synthesis of 1D ZnO-MMNTs

In a typical procedure, 10 ml deionized water and 10 ml absolute ethyl alcohol were dissolved together under stirring. Then 0.742 g zinc nitrate was added into the mixed solution with stirring until clear. After dissolution, silk was dipped into the precursor solution and soaked about 12 h. Finally, the silk was dried at 200 °C and annealed at 600 °C for 2 h in air.

2.3. Fabrication of enzymatic biosensor

The GOx enzymes were successfully immobilized in the ZnO-MMNTs by electrostatic adsorption interaction and the CHIT-assisted cross-linking technique. Firstly, GOx enzymes solution (10.0 mg ml^{-1}) was prepared by dissolving GOx in 0.01 M phosphate buffer saline (PBS pH=7.4), and 0.5 wt% CHIT (molar weight ~1×10^6, 75–85% deacetylation) solution was prepared by dissolving CHIT in acetic acid solution. 1 mg ZnO-MMNTs were added into 10 μL GOx solution and left for 15 min. Then the compounds were deposited onto the surface of a SiO_2 chip (3 mm × 1 cm) coated with an exposed Au film (3 mm × 3 mm). After drying in air, the CHIT solution was further applied onto the electrode surface to prevent possible enzyme leakage. Then the device was dried at 4 °C overnight in a refrigerator, followed by washing step to remove the unimmobilized GOx.

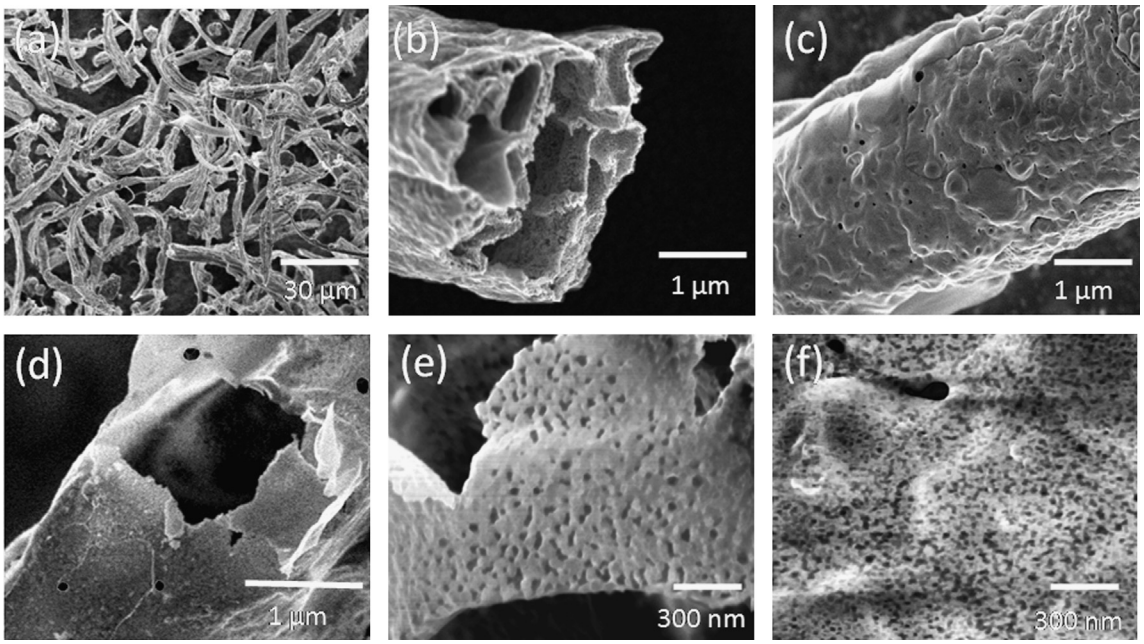

Fig. 1. SEM images of the as-prepared ZnO-MMNTs. (a) A lower magnification image of the ZnO-MMNTs. (b) Multiwall tubes based structure viewed from the longitudinal section of the ZnO-MMNTs. (c) Overview of the outer surface of a single ZnO-MMNT, a number of pores about several hundred nanometers are scattered. (d) Hollow structure viewed from a break in the outer tube. (e) Mesoporous structure of the single inner wall. (f) Mesoporous structure of the outer wall, large pores about several hundred nanometers still exist.

3. Results and discussion

3.1. Characterization of the ZnO-MMNTs

The SEM images of the as-synthesized ZnO-MMNTs are shown in Fig. 1. From a low-magnified image (Fig. 1a), we can see that the product is composed of nanotubes with length about hundreds of micrometers and diameter about 2–3 μm. The structure of multi-wall nanotubes is shown in Fig. 1b, it is observed that several inner tubes about hundreds of nanometers in diameter are distributed in a single outer tube. The inner tubes are built by multilayer porous walls (~50–200 nm in thickness), and plenty of mesopores are located in the walls (Fig. 1e). The outer wall (~50–200 nm in thickness) not only has numerous mesopores (Fig. 1f), but also has a few of scattered large pores (~100 nm) (Fig. 1c, d). The break of the tube shows a hollow structure of the ZnO-MMNTs (Fig. 1d).

The schematic structural characteristics of ZnO-MMNTs for biosensing are shown in Fig. 2. Because of the scale of mesopores (~20–50 nm) in the walls is larger than that of GOx (~10–20 nm), the enzymes can be adsorbed into the pores through physical and electrostatic adsorption interactions (Zhao et al., 2013a, 2013b). Due to the increased specific surface resulting from the widely distributed pores, the active surface area available for enzymes binding was thus enhanced (Lee et al., 2005). Furthermore, the porous environment also provides suitable room for the extending of enzyme molecules and would retain the essential secondary structure of the entrapped protein (Fig. 2b). Therefore, the mesoporous structures can afford high enzymes loading without serious loss of activity and result in high catalysis efficiency. In addition, the inner tubes can provide convenient channels for fast diffusion of reactants, and the 1D structured ZnO walls benefit the electrons transport, as illustrated in Fig. 2a. Both channels are crucial for fast response of the biosensor.

A typical XRD pattern of the ZnO-MMNTs is shown in Fig. S1a. All the diffraction peaks can be indexed as the wurtzite structure ZnO in the standard data (JCPDS 36-1451). The sharp peaks and strong intensity reveal a high crystallographic quality. Average grain size of the sample was calculated as 26 nm according to Scherrer's formula. The typical Raman spectra in the range of 200–700 cm^{-1} are shown in Fig. S1b. Three peaks at 332, 439, and 582 cm^{-1} are corresponding to the wurtzite structure ZnO E_{2H}–E_{2L}, E_{2H} and E_{1L} modes, respectively. The E_{2H} mode involving only oxygen atoms articulates that the nanotubes are of high-quality crystal. The presence of weak E_{1L} mode suggests the formation of defects (oxygen vacancies or zinc interstitials) (Zhao et al., 2013a, 2013b).

3.2. Electrochemical characteristics of the enzymatic biosensor

The electrochemical characterization of the biosensor was investigated by cyclic voltammetry (CV) in PBS (pH=7.4) at scan rate of 0.1 V s^{-1}. The typical CV curves of the biosensor in the absence and presence of 1 mM glucose are shown in Fig. S2a. It is observed that the CHIT/GOx/ZnO-MMNTs/Au electrode presents clear electrochemical behavior with a pair of typical oxidation and reduction peaks in the absence of glucose. The control experiment (Fig. S3) demonstrated that the redox peaks were assigned to PBS (Ahmad et al., 2010). However, when the glucose was added, the reduction current was suppressed while the oxidation current increased significantly, which indicated the oxidation of glucose by GOx (Kong et al., 2009). The result indicates that the ZnO-MMNTs were successfully used as matrix to hold enzymes and the immobilized GOx exhibited fine electro-catalytic activity to glucose. All the above illustrate that the enzymes were effectively immobilized and well biological activity was kept.

To further investigate the characteristics of ZnO-MMNTs based enzymatic electrode, the effect of scan rate on the voltammetric behavior was also studied. As is shown in Fig. S2b, the oxidation peak currents increase and peak potentials shift positively with the increase of scan rates. The anodic current increase is almost linear versus the square root of scan rate (correlation coefficient R=0.9968) as shown in the inset of Fig. 3b. All these results indicate a surface diffusion controlled process (Zhang and Dong, 2004).

3.3. Application as a glucose biosensor

The steady-state amperometric response of the glucose biosensor was investigated by successively adding the same amount of glucose into stirring PBS. As shown in Fig. 3a, the biosensor exhibited rapid and sensitive response to the addition of glucose. The current increases with the increase of glucose

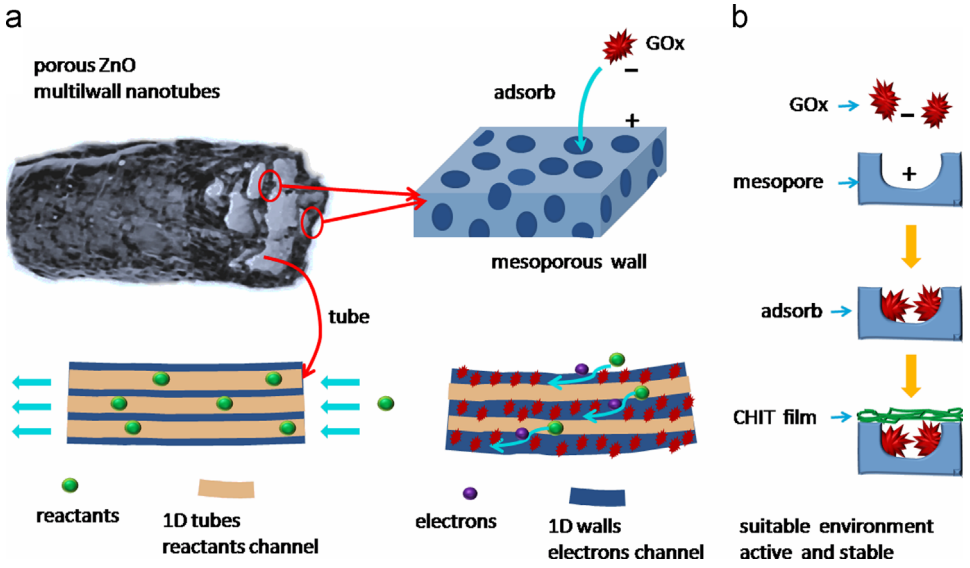

Fig. 2. Schematic illustration of the features of the ZnO-MMNTs for immobilizing the redox enzyme GOx. (a) The mesopores in the wall for holding GOx enzyme molecules; the 1D channels for reactants diffusion and electrons transport. (b) The GOx immobilization process: entering the mesopore by physical and electrostatic adsorption and then entrapped by the permeable CHIT membrane. Scale-adaptive cell is afforded for maintaining activity and stability.

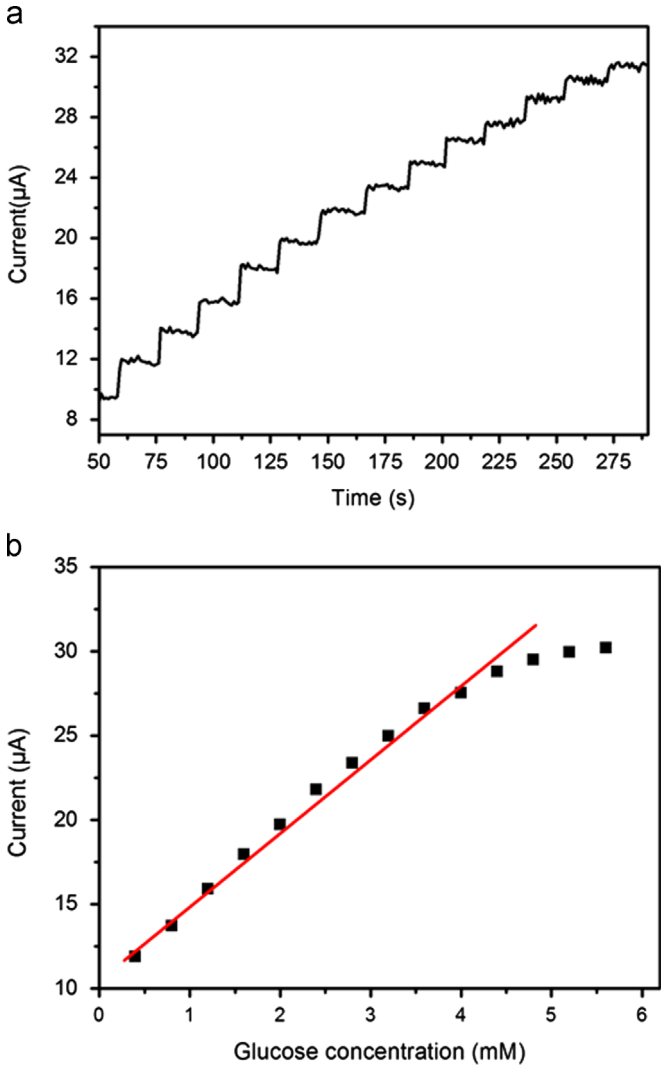

Fig. 3. Real time electronic response of biosensor to glucose. The current is measured as a function of time in PBS. The applied voltage is 600 mV. (a) Typical current–time response curve for successive addition of glucose with a step of 0.4 mM under stirring. (b) The calibration curve of the glucose concentration versus current.

concentration step by step and achieved 95% of the steady-stated current within 2 s. The corresponding calibration curve of response to glucose concentration is shown in Fig. 3b. It is found that the current increases with the increasing glucose concentration at a large linear slope from 0.02 to 4.4 mM (correction coefficient $R=0.997$). The linear regression equation is the following: $I\,(\mu A)=10.77+4.306C$ (mM). This kind of biosensor presents a high sensitivity of 47.2 $\mu A\,mM^{-1}\,cm^{-2}$ and a low detection limit of 10 μM (based on the signal-to-noise (S/N) of 3). Compared with other ZnO nanostructures, the ZnO-MMNTs modified electrode have better performance in sensitivity and response time (Table S1). All the above indicate a good electrocatalytic oxidative and very fast electron exchange behavior of the biosensor, due to the mesoporous structure for higher enzyme loading, compatible microenvironment for maintaining its bioactivity, and special channels for reactants and electrons transport.

To evaluate the biological activity of the immobilized GOx, the apparent Michaelis–Menten constant K_M^{app} is generally calculated from the Lineweaver–Burk equation

$$1/i = (K_M^{app}/i_{max})(1/C) + 1/i_{max}$$

where C is the glucose concentration, i_{max} and i are the currents measured for enzymatic product detection under conditions of substrate saturation and steady state, respectively. According to the Lineweaver–Burk plot, the K_M^{app} was calculated to be 1.09 mM, which is much lower than many other matrices (Table S1). This low K_M^{app} indicates that good bioactivity of the immobilized GOx was maintained.

Selectivity to target analyte is an important analytical factor for an amperometric biosensor. The interference test was carried out by adding the possible interfering species, including uric acid (UA), ascorbic acid (AA) and dopamine (DA). It is observed that the addition of these potential interferents do not substantially change the response signal (Fig. S4). It indicates excellent selectivity of the biosensor toward glucose detection.

The stability of the biosensor was measured by monitoring the response after successively cycling the electrode, it is found that the response is almost unchanged after 20 circles. The long term stability was investigated after four weeks storage at 4 °C, and almost 90% of its initial value was remained. The high stability of the modified electrode can be attributed to the mesoporous nanowalls, which provide scale-adaptive pores for holding GOx and friendly microenvironment for retaining their activity (Fig. 2b). What is more, the protecting effect of the permeable CHIT membrane formed on the surface of the mesoporous nanowalls and the strong electrostatic interaction with GOx molecules also play important roles in the stability of the biosensor.

The ZnO-MMNTs are promising material for commercial glucose sensor devices. Firstly, silk is abundant and inexpensive. Secondly, the fabrication of ZnO-MMNTs by replicating silk is simple, facile, low cost and suitable for mass production. The sensor can be fabricated by simply pasting the material on an electrode. Finally, the biosensor has long term stability.

4. Conclusions

In summary, ZnO-MMNTs were prepared by a simple and facile replication of silk. The advantages of employing the ZnO-MMNTs to successfully assemble GOx were demonstrated. The mesporous multiwalls provide scale-adaptive cell for assembling GOx and specific surface for electrical communication. The 1D multiwall nanotubes act as an excellent channels for reactants and electrons transport. The as-fabricated biosensor show high sensitivity, fast response, low detection limit, high anti-interferent and good stability. These results demonstrate that ZnO-MMNTs are an attractive platform for the fabrication of efficient enzymatic biosensors.

Acknowledgments

This work was partly supported by the National Natural Science Foundation of China and the Doctorate Fund of the Ministry of Education.

Appendix A. Supporting information

Supplementary data associated with this article can be found in the online version at http://dx.doi.org/10.1016/j.bios.2013.05.017.

References

Ahmad, M., Pan, C.F., Luo, Z.X., Zhu, J., 2010. Journal of Physical Chemistry C 114, 9308–9313.
Becerril, H.A., Stoltenberg, R.M., Wheeler, D.R., Davis, R.C., Harb, J.N., Woolley, A.T., 2005. Journal of the American Chemical Society 127, 2828–2829.

Belcher, A.M., Wu, X.H., Christensen, R.J., Hansma, P.K., Stucky, G.D., Morse, D.E., 1996. Nature 381, 56–58.
Brutchey, R.L., Yoo, E.S., Morse, D.E., 2006. Journal of the American Chemical Society 128, 10288–10294.
Cha, J.N., Stucky, G.D., Morse, D.E., Deming, T.J., 2000. Nature 403, 289–292.
Chi, Q., Zhang, J.D., Dong, S.J., Wang, E., 1994. Journal of the Chemical Society Faraday Transactions 90, 2057–2060.
Deng, L., Liu, Y., Yang, G.C., Shang, L., Wen, D., Wang, F., Xu, Z.A., Dong, S.J., 2007. Biomacromolecules 8, 2063–2071.
Dickerson, M.B., Sandhage, K.H., Naik, R.R., 2008. Chemical Reviews 108, 4935–4978.
Fang, B., Zhang, C.H., Wang, G.F., Wang, M.F., Ji, Y.L., 2011. Sensors and Actuators B 155, 304–310.
Fatemi, H., Khodadadi, A.A., Firooz, A.A., Mortazavi, Y., 2012. Current Applied Physics 12, 1033–1038.
Heller, A., 1990. Accounts of Chemical Research 23, 128–134.
Huang, J.Y., Wang, X.D., Wang, Z.L., 2006. Nano Letters 6, 2325–2331.
Kong, T., Chen, Y., Ye, Y.P., Zhang, K., Wang, Z.X., Wang, X.P., 2009. Sensors and Actuators B 138, 344–350.
Lee, D., Lee, J., Kim, J., Na, H.B., Kim, B., Shin, C.H., Kwak, J.H., Dohnalkova, A., Grate, J. W., Hyeon, T., Kim, H.S., 2005. Advanced Materials 17, 2828–2833.
Lei, Y., Yan, X.Q., Zhao, J., Liu, X., Song, Y., Luo, N., Zhang, Y., 2011. Colloids and Surfaces B 82, 168–172.
Luo, X.L., Xu, J.J., Du, Y., Chen, H.Y., 2004. Analytical Biochemistry 334, 284–289.
Naik, R.R., Stringer, S.J., Agarwal, G., Jones, S.E., Stone, M.O., 2002. Nature Materials 1, 169–172.
Nuraje, N., Dang, X.G., Qi, J.F., Allen, M.A., Lei, Y., Belcher, A.M., 2012. Advanced Materials 24, 2885–2889.
Nuraje, N., Su, K., Haboosheh, A., Samson, J., Manning, E.P., Yang, N.l., Matsui, H., 2006. Advanced Materials 18, 807–811.
Pan, L.J., Yu, D.Y., Zhai, D.Y., Lee, H.R., Zhao, W.T., Liu, N., Wang, H.L., Tee, B.C.K., Shi, Y., Cui, Y., Bao, Z.N., 2012. Proceedings of the National Academy of Sciences 109, 9287–9292.
Rakow, N.A., Suslick, K.S., 2000. Nature 406, 710–714.
Riklin, A., Katz, E., Willner, I., Stocker, A., Buchmann, A.F., 1995. Nature 376, 672–675.
Selbach, S.M., Einarsrud, M.A., Tybell, T., Grande, T., 2007. Journal of the American Ceramic Society 90, 3430–3434.
Singh, S.P., Arya, S.K., Pandey, P., Malhotra, B.D., Saha, S., Sreenivas, K., Gupta, V., 2007. Applied Physics Letters 91, 63901–63903.
Tao, A.R., Niesz, K., Morse, D.E., 2010. Journal of Materials Chemistry 20, 7916–7923.
Xie, J.N., Wang, S.Y., Aryasomayajula, L., Varadan, V.K., 2007. Nanotechnology 18, 065503.
Zang, J.F., Li, C.M., Cui, X.Q., Wang, J.X., Sun, X.W., Dong, H., Sun, C.Q., 2007. Electroanalysis 19, 1008–1014.
Zhai, D.Y., Liu, B.R., Shi, Y., Pan, L.J., Wang, Y.Q., Li, W.B., Zhang, R., Yu, G.H., 2013. ACS Nano 7, 3540–3546.
Zhai, Y.L., Zhai, S.Y., Chen, G.F., Zhang, K., Yue, Q.L., Wang, L., Liu, J.F., Jia, J.B., 2011. Journal of Electroanalytical Chemistry 656, 198–205.
Zhang, L., Dong, S., 2004. Journal of Electroanalytical Chemistry 568, 189–194.
Zhao, M., Huang, J.Y., Zhou, Y., Chen, Q., Pan, X.H., He, H.P., Ye, Z.Z., 2013a. Biosensors and Bioelectronics 43, 226–230.
Zhao, M., Wang, X.C., Cheng, J.P., Zhang, L.W., Jia, J.F., Li, X.J., 2013b. Current Applied Physics 13, 403–407.
Zhao, W., Xu, J.J., Shi, C.G., Chen, H.Y., 2005. Langmuir 21, 9630–9634.
Zhu, X.L., Yuri, I., Gan, X., Suzuki, I., Li, G.X., 2007. Biosensors and Bioelectronics 22, 1600–1604.